JOURNAL OF VIROLOGY, Feb. 2011, p. 1747–1756 Vol. 85, No. 4
0022-538X/11/$12.00 doi:10.1128/JVI.01428-10

Characterization of Two Substrains of Puumala Virus That Show Phenotypes That Are Different from Each Other and from the Original Strain[▽]

Karin B. Sundström,[1,2,3] Malin Stoltz,[1,3] Nina Lagerqvist,[1,2] Åke Lundkvist,[1,2] Kirill Nemirov,[2,4] and Jonas Klingström[1,3]*

Department of Microbiology, Tumor and Cell Biology, Karolinska Institutet, SE-171 77 Stockholm, Sweden[1]; Department of Virology[2] and Centre for Microbiological Preparedness,[3] Swedish Institute for Infectious Disease Control, SE-171 82 Solna, Sweden; and INSERM, U758, IFR 128, Filovirus Laboratory, 21 Avenue Tony Garnier, Lyon F-69007, France[4]

Received 8 July 2010/Accepted 11 November 2010

Hantaviruses, the causative agents of two emerging diseases, are negative-stranded RNA viruses with a tripartite genome. We isolated two substrains from a parental strain of Puumala hantavirus (PUUV-Pa), PUUV-small (PUUV-Sm) and PUUV-large (PUUV-La), named after their focus size when titrated. The two isolates were sequenced; this revealed differences at two positions in the nucleocapsid protein and two positions in the RNA-dependent RNA polymerase, but the glycoproteins were identical. We also detected a 43-nucleotide deletion in the PUUV-La S-segment 5′ noncoding region covering a predicted hairpin loop structure that was found to be conserved among all hantaviruses with members of the rodent subfamily Arvicolinae as their hosts. Stocks of PUUV-La showed a lower ratio of viral RNA to infectious particles than stocks of PUUV-Sm and PUUV-Pa, indicating that PUUV-La replicated more efficiently in alpha/beta interferon (IFN-α/β)-defective Vero E6 cells. In Vero E6 cells, PUUV-La replicated to higher titers and PUUV-Sm replicated to lower titers than PUUV-Pa. In contrast, in IFN-competent MRC-5 cells, PUUV-La and PUUV-Sm replicated to similar levels, while PUUV-Pa progeny virus production was strongly inhibited. The different isolates clearly differed in their potential to induce innate immune responses in MRC-5 cells. PUUV-Pa caused stronger induction of IFN-β, ISG56, and MxA than PUUV-La and PUUV-Sm, while PUUV-Sm caused stronger MxA and ISG56 induction than PUUV-La. These data demonstrate that the phenotypes of isolated hantavirus substrains can have substantial differences compared to each other and to the parental strain. Importantly, this implies that the reported differences in phenotypes for hantaviruses might depend more on chance due to spontaneous mutations during passage than inherited true differences between hantaviruses.

Hantaviruses are the causative agents for two severe and often fatal human diseases, hemorrhagic fever with renal syndrome (HFRS) and hantavirus cardiopulmonary syndrome (HCPS), for which there are currently no approved treatments or vaccines available (47, 51). The natural hosts for hantaviruses are rodents, insectivores, and talpids, although so far only rodent-borne hantaviruses have been shown to cause disease in humans (5, 47, 51). Like the other viruses within the *Bunyaviridae* family, hantaviruses have a tripartite negative-stranded RNA genome consisting of the small (S), medium (M), and large (L) segments. Hantavirus produces four structural proteins, the nucleocapsid (N) protein (S segment), the envelope glycoprotein (G) precursor, which after cleavage forms the Gn and Gc proteins (M segment), and the RNA-dependent RNA polymerase (RdRp) (L segment) (47). In several, but not all, hantaviruses, there is also an alternative open reading frame (ORF) in the S segment that might encode a small nonstructural protein (NSs) (20).

In natural hosts, hantaviruses establish lifelong infection, replicate, and spread without causing obvious harm (9). In contrast, infection of humans can cause HFRS or HCPS. Why infection of humans, and not the natural hosts, causes disease is unknown. It is under debate whether human disease is caused by the virus and/or by host-mediated factors (reviewed in references 32 and 47). Hantavirus research is dependent on cell line-adapted strains for infectious experiments *in vitro*. Wild-type viruses do not readily infect cells, and hence cannot be propagated *in vitro*, and at this time, there is no reverse genetics system available for the construction of recombinant viruses. As hantaviruses are isolated and passaged in cell lines, most often on the alpha/beta interferon (IFN-α/β)-defective African green monkey kidney epithelial Vero E6 cell line, substrains that would not survive in a natural host might evolve. Hence, there is a risk that infectious experiments with a virus stock containing such substrains can yield results that, at least partly, might not necessarily reflect natural infection in hosts or patients.

We hypothesized that natural mutations accumulating during passage of hantaviruses might give rise to substrains with phenotypes that are different from each other and also from the original strain. When titrating a stock of Puumala virus (PUUV) strain Kazan-E6 (PUUV strain Kazan adapted to Vero E6 cells) (31) on Vero E6 cells, we observed clear differences in focus size, indicating that subspecies with different phenotypes had evolved. From the PUUV focuses, we isolated virus causing large (PUUV-La) and small (PUUV-Sm) fo-

* Corresponding author. Mailing address: Centre for Microbiological Preparedness, Swedish Institute for Infectious Disease Control, SE-171 82 Solna, Sweden. Phone: 46 8 457 23 50. Fax: 46 8 30 79 57. E-mail: Jonas.Klingstrom@smi.se.

▽ Published ahead of print on 24 November 2010.

cuses. The two isolated substrains were sequenced, and compared to each other, they were found to contain several differences in the S and L segments, including two amino acid changes in N and RdRp, and a large deletion in PUUV-La S-segment 5′ noncoding region (5′ NCR), but identical M segments. The isolation of these two substrains gave us the opportunity to study possible phenotypic differences between closely related substrains of a hantavirus and to compare purified substrains with the parental PUUV Kazan-E6 strain (hereafter called parental PUUV [PUUV-Pa]) that is likely a mixture of several different substrains. In order to analyze the phenotypes, we studied the kinetics of viral replication after infection of IFN-α/β-defective Vero E6 cells (7) and the kinetics of viral replication and induction of innate immune responses after infection of the IFN-competent human fibroblast cell line MRC-5. We report that hantavirus substrains can, compared to each other and compared to the parental strain, show surprisingly different phenotypes on different cell types.

MATERIALS AND METHODS

Cells and viruses. The African green monkey kidney epithelial cell line Vero E6, human fetal lung fibroblast cell line MRC-5, and PUUV strain Kazan-E6 (called PUUV-Pa in this report) (31) were used in the study. Vero E6 cells were grown in Dulbecco's modified Eagle's medium supplemented with 5% fetal bovine serum (FBS), 20 mm HEPES, 100 U of penicillin/ml, and 100 μg of streptomycin/ml. MRC-5 cells were grown in minimum essential medium supplemented with 10% FBS, 100 U of penicillin/ml, and 100 μg of streptomycin/ml. All reagents were from Invitrogen, Carlsbad, CA.

Propagation and titration of PUUV were performed on Vero E6 cells as previously described (24).

Focus purification of PUUV substrains. To purify single viruses, PUUV-Pa (previously passaged 24 times on Vero E6 cells, each time for 2 weeks) with a titer of 100,000 focus-forming units (FFU) per ml was diluted to approximately 5 FFU/ml (the dilution medium consisted of Hanks balanced salt solution supplemented with 2% HEPES, 2% FBS, 100 U of penicillin/ml, and 100 μg of streptomycin/ml [all reagents from Invitrogen]). Then, confluent Vero E6 cells in 24-well plates were infected with 0.2 ml of diluted virus/well. After adsorption for 1 h at 37°C, the cells were overlaid with basal 0.5% agarose medium. Seven days later, the agarose medium was removed, and the cells were incubated with 0.5 ml of dilution medium per well for 1 h at 37°C. The supernatant was then collected, and the cells were fixed and stained as previously described (24). Supernatant from wells containing a single focus was propagated on Vero E6 cells, and the procedure was repeated one more time for each of the two substrains isolated.

Amplification and sequencing. To compare the genomic sequences of PUUV-La and PUUV-Sm, total RNA was extracted from the supernatants of infected Vero E6 cells and subjected to several rounds of reverse transcription-PCR (RT-PCR) with primers specific for different segments of PUUV (strain Kazan) (31, 37). All reactions were performed with SuperScript III reverse transcriptase enzyme (Invitrogen), and all amplifications were performed with *Pfu* Ultra Fusion (Stratagene, Agilent Technologies Inc., Santa Clara, CA). The S-segment sequences were amplified in a single RT-PCR. The M and L genomic segments were each reverse transcribed and amplified in three overlapping parts: nucleotides (nt) 1 to 1300, nt 1141 to 2504, and nt 2400 to 3682 (M segment) and nt 1 to 2248, nt 2152 to 4349, and nt 4226 to 6550 (L segment). All amplified fragments were separated in agarose gels, purified with MinElute gel extraction kit (Qiagen, Hilden, Germany), and subjected to direct sequencing on an ABI 3100 (Applied Biosystems, Foster City, CA) with Big Dye Terminator cycle sequencing kit v3.1.

Analyses of RNA secondary structure. The predicted secondary structures of the complete S-segment 5′ NCR for various hantaviruses were rendered using CONTRAfold (8), a program that predicts the secondary structure of RNA using a method based on conditional log linear models. The sequences used for predictions were obtained from the Nucleotide database at the National Center for Biotechnology Information (NCBI) (GenBank accession numbers shown in parentheses) as follows: Amur virus (AB127997), Andes virus (NC_003466), Dobrava virus (L41916), Hantaan virus (AF321095), Khabarovsk virus (U35255), Muju virus (DQ138140), Prospect Hill virus (U47136), PUUV (AY526219), Saaremaa virus (AJ616854), Seoul virus (AF406965), Sin Nombre virus (L25784), Thottapalayam virus (NC_010704), Topografov virus (AJ011646), and Tula virus (AF063897).

Indirect immunofluorescence assay (IFA). Vero E6 cells seeded on coverslips in 24-well plates were infected when the cells were confluent, and 4 days later, they were fixed in ice-cold acetone-methanol (1:1) for 10 min at −20°C and then air dried. Staining was performed with either convalescent human anti-PUUV serum (1:40 dilution), followed by a fluorescein isothiocyanate (FITC)-conjugated goat anti-human IgG (Sigma-Aldrich, St. Louis, MO) (1:50 dilution), or with a PUUV N-specific monoclonal antibody (MAb) 1C12 (1:50 dilution) (30), followed by FITC-conjugated anti-mouse antibody (Sigma-Aldrich). Nuclei were stained with 4′,6′-diamidino-2-phenylindole (DAPI) (Sigma-Aldrich) (1:1,000 dilution). The resulting images were visualized by Nikon Eclipse TE300 and Wasabi imaging software, version 1.5 (Hamamatsu, Herrsching am Ammersee, Germany).

Immunoblot analysis. The samples were homogenized in lysis buffer (50 mM Tris, 150 mM NaCl, 2 mM EDTA, and 1% NP-40 [pH 7.6]) supplemented with Complete protease inhibitor cocktail minitablets (Roche Diagnostics, Mannheim, Germany). The lysates were mixed 1:4 with NuPAGE 4× LDS sample preparation buffer (Invitrogen), resolved on 10% NuPAGE Novex Bis-Tris gel (Invitrogen), and transferred to a nitrocellulose membrane. Blocking was performed overnight at 4°C in phosphate-buffered saline (PBS) supplemented with 5% nonfat dry milk and 0.1% Tween 20. The membranes were subsequently incubated with anti-N MAb 1C12 (1:500 dilution) or with convalescent human anti-PUUV serum (1:100 dilution) for 1 h at room temperature, followed by horseradish peroxidase (HRP)-conjugated anti-mouse IgG (Bio-Rad, Hercules CA) (1:5,000 dilution) or HRP-conjugated anti-human IgG (Bio-Rad) (1:5,000 dilution). Proteins were detected with ECL Plus Western blotting detection kit (GE Healthcare, Buckinghamshire, United Kingdom) following the manufacturer's protocol.

RNA preparation and RT-PCR. Total RNA from infected or mock-infected cells or from supernatant was isolated using TriPure isolation reagent (Roche Diagnostics). To remove any contaminating DNA, RNA was treated with Turbo DNA-free DNase (Ambion, Austin, TX). cDNA synthesis was performed using SuperScript III reverse transcriptase (Invitrogen), random primers (Invitrogen), and RNaseOUT recombinant RNase inhibitor (Invitrogen).

Quantitative real-time PCR. Quantification of ISG56, IFN-β, and β-actin mRNA was performed using TaqMan gene expression assays (Applied Biosystems). The TaqMan minor groove binder (MGB) probe and primers (Applied Biosystems) were used as described earlier for quantification of MxA (22) and for quantification of PUUV S-segment RNA (23). The quantitative real-time PCR (Q-PCR) was performed using ABI7900 HT Fast sequence detection system (Applied Biosystems) with software SDS version 2.3. Data were normalized to β-actin data and presented as the change in induction relative to that of noninfected control cells.

To obtain a reference when quantifying PUUV S-segment RNA in virus stocks, stocks were diluted to 100,000 FFU/ml and mixed with a fixed amount of human cells before RNA was extracted. Human β-actin was then used as a reference gene when calculating the levels of PUUV S-segment RNA in the samples.

Statistics. Factorial analysis of variance (ANOVA) was calculated using Statistica version 9 (StatSoft Inc., Tulsa, OK).

RESULTS

Isolation and purification of PUUV substrains. There is currently nothing known regarding the possible effect of substrains within a hantavirus strain on the overall phenotype of the strain or whether closely related hantavirus substrains might have different phenotypes or not. When a stock of PUUV-Pa (earlier passaged 24 times on Vero E6 cells) was titrated, we observed focuses of clearly different sizes (Fig. 1A), indicating that subspecies with phenotypic differences had evolved during passaging of PUUV-Pa. We therefore subcloned one isolate from a large focus (PUUV-La) and one from a small focus (PUUV-Sm) from the parental PUUV-Pa stock on Vero E6 cells and further purified the isolates by subcloning them one more time on Vero E6 cells in order to analyze possible differences in the phenotypes (possible differ-

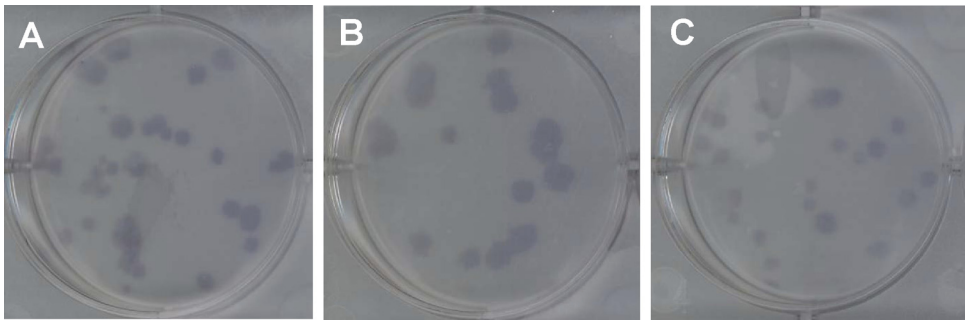

FIG. 1. Focus size of PUUV-Pa, PUUV-La, and PUUV-Sm. Vero E6 cells were infected with PUUV-Pa (A), PUUV-La (B), and PUUV-Sm (C) and then overlaid with agarose medium for 7 days. The cells were fixed and incubated with convalescent anti-PUUV serum, followed by HRP-conjugated anti-human IgG, and staining with 3,3′,5,5′-tetramethylbenzidine (TMB). The photos show virus-infected cells that are representative of three or more independent experiments, each with two or more replicates.

ences between the phenotypes for the two substrains and the phenotype of the parental strain).

When titrated, PUUV-La (Fig. 1B) generally showed larger focuses than PUUV-Sm (Fig. 1C), suggesting that PUUV-La had replicated and/or spread more efficiently than PUUV-Sm in Vero E6 cells.

Genetic characterization of the two isolates. In order to analyze possible differences at the nucleotide level in the two substrains, they were both sequenced. We isolated RNA from supernatants in order to sequence RNA from virus particles. Except for the outer 3′ and 5′ parts, the two substrains were successfully sequenced (S segment [nt 22 to 1806], M segment [nt 26 to 3656], and L segment [nt 27 to 6524]). For a reference sequence, we used the previously reported sequence for PUUV Kazan adapted to Vero E6 cells (31, 37). Several differences in the nucleotide sequences for the two isolates were observed, indicating that they both had gone through several rounds of mutations that had not caused visible differences in focus size when earlier stocks of PUUV-Pa had been titrated.

The structural proteins differed at four positions in the two isolates. They showed one amino acid difference each in the N protein compared to the original PUUV-Pa sequence. Interestingly, both mutations occurred at aspartic acid residues, suggesting that both these aspartic acids are not absolutely required for hantavirus replication, although they are in an area of the N protein with four well-conserved aspartic acids (Table 1). For PUUV-La, we observed a D27E mutation and for PUUV-Sm, we observed a D35Y mutation in an otherwise highly conserved region of the N protein (Table 1).

We also observed two mutations causing amino acid substitutions in the RdRp; a L611F mutation in PUUV-Sm and a P702S mutation in PUUV-La, both detected in highly conserved regions of RdRp (Tables 2 and 3).

Besides the ORF coding for the N protein, the S segment also contains an alternative ORF, possibly encoding an NSs (20), which overlaps with the N-protein ORF. In total, three differences compared to PUUV-Pa were observed for NSs: a W21C mutation in PUUV-Sm, and a M14R and a C55Y mutation in PUUV-La. Notably, the PUUV-La N-protein D27E mutation and NSs protein M14R mutation are caused by one point mutation in the PUUV-La S segment, and the PUUV-Sm N protein D35Y and NSs protein W21C mutations are also caused by one point mutation in the PUUV-Sm S segment.

Several silent mutations were also observed in PUUV-La and PUUV-Sm. In the S segment, PUUV-Sm has a U inserted at position 22 in the 3′ NCR. As previously observed (37, 41), there seems to be a "hot spot" of mutations around position 1570 in the PUUV S-segment 5′ NCR; a G1569A mutation was observed in PUUV-La and a U1577G mutation in PUUV-Sm. The most pronounced difference detected was a 43-nucleotide-long part of the 5′ NCR that was missing in the PUUV-La S segment. Interestingly, this stretch of nucleotides forms a distinct secondary structure in the form of a hairpin loop (Fig. 2). Furthermore, a silent A2706G mutation was detected in the PUUV-La L segment, while the M segments were identical for PUUV-La and PUUV-Sm.

A conserved hairpin loop RNA structure is missing in PUUV-La. As the 43-nucleotide deletion observed in PUUV-La was predicted to form a distinct secondary structure (Fig. 2), we looked at whether this structure was a common feature of other hantaviruses as well. The complete 5′ NCRs for various

TABLE 1. Hantavirus N-protein sequences from amino acids 20 to 40[a]

Virus[b]	N-protein sequence (aa 20 to 40)[c]
PUUV-Pa	VARQKLKDAERAVEVDPDDVN
PUUV-La	VARQKLK**E**AERAVEVDPDDVN
PUUV-Sm	VARQKLKDAERAVEV**Y**PDDVN
PUUV Sotkamo	VARQKLKDAERAVEVDPDDVN
PUUV Umeå	VARQKLKDAEKAVEMDPDDVN
ANDV	TARQKLKDAEKAVEVDPDDVN
SNV	TARQKLKDAERAVELDPDDVN
HTNV	IARQKVRDAEKQYEKDPDELN
SEOV	IARQKVKDAEKQYEKDPDDSN

[a] Sequences were obtained from GenBank (accession numbers shown in parentheses) as follows: PUUV-Pa (PUUV strain Kazan; accession no. CAB06337.1), PUUV strain (NP_941984), PUUV strain Umeå (AAS19474), Andes virus (NP_604471), Sin Nombre virus (AAA75529), Hantaan virus (AAG53970), and Seoul virus (AAK96243).

[b] PUUV Sotkamo, PUUV strain Sotkamo; PUUV Umeå, PUUV strain Umeå; ANDV, Andes virus: SNV, Sin Nombre virus; HTNV, Hantaan virus; SEOV, Seoul virus.

[c] The amino acid sequences are shown from amino acids (aa) 20 to 40. The mutations observed in the PUUV-La and PUUV-Sm N proteins are shown in boldface type.

TABLE 2. Hantavirus RdRp sequences from amino acids 601 to 620[a]

Virus	RdRp sequence (aa 601 to 620)[b]
PUUV-Pa	LRSVFAFHFLLSTSQKMKLC
PUUV-La	LRSVFAFHFLLSTSQKMKLC
PUUV-Sm	LRSVFAFHFL**F**STSQKMKLC
PUUV Sotkamo	LRSVFAFHFLLSVSQKMKLC
PUUV Umeå	LRSVFAFHFLLSPSQKMKLC
ANDV	LRSIFSFHFLLCVSQKMKLC
SNV	LRSVFSFHFLLCVSQKMKIC
HTNV	IRSVFANHFLLAICQKMKLC
SEOV	IRSVFAYHFLLAICQKMKLC

[a] Sequences were obtained from GenBank (accession numbers shown in parentheses) as follows: PUUV-Pa (PUUV strain Kazan; accession no. ABN51178), PUUV strain Sotkamo (NP_942587), PUUV strain Umeå (AAS19472), ANDV (NP_604473), SNV (AAC42204), HTNV (NP_941982), and SEOV (NP_942558).

[b] The mutation observed in PUUV-Sm RdRp is shown in boldface type.

hantaviruses were analyzed *in silico* for secondary RNA structure (8). Interestingly, the results showed that the predicted hairpin loop lacking in PUUV-La is conserved for PUUV and other Arvicolinae-borne hantaviruses like Khabarovsk virus, Topografov virus, Tula virus, and Prospect Hill virus but is not found in hantaviruses that have species of Murinae (for example, Hantaan virus, Seoul virus, and Dobrava virus) or Sigmodontinae (for example, Sin Nombre virus and Andes virus) as hosts (data not shown). Thus, it seems that the secondary structure of this part of the 3′ NCR in the S segment is well conserved among PUUV and other Arvicolinae-borne hantaviruses but that it is not an absolute requirement for hantaviruses in general.

PUUV-Sm constitutes a minor part of PUUV-Pa. The N-terminal region of PUUV N protein is recognized by MAb 1C12 (30). In order to test whether MAb 1C12 could recognize the mutated forms of N protein, we infected Vero E6 cells with the different isolates and then used MAb 1C12 as the detection MAb in immunofluorescence microscopy. While PUUV-Pa- and PUUV-La-infected cells were clearly detected using MAb 1C12, PUUV-Sm-infected cells could not be identified (Fig. 3A). However, like PUUV-La- and PUUV-Pa-infected cells, PUUV-Sm-infected cells could be identified using a polyclonal human anti-PUUV convalescent-phase serum (Fig. 3A). A similar pattern was observed when MAb 1C12 was used for detection of N protein on Western blots: a clear band of the expected size was observed for PUUV-La and for PUUV-Pa, but no band was observed for PUUV-Sm (Fig. 3B). However, when a polyclonal human HFRS convalescent-phase serum was also used, PUUV-Sm N protein could be detected (Fig. 3B). Thus, it can be concluded that the D35 amino acid is important for binding of MAb 1C12 to the PUUV N protein.

As MAb 1C12 did not recognize PUUV-Sm N protein, we could indirectly analyze the proportion of PUUV-Sm in PUUV-Pa. Vero E6 cells were infected with 50 FFU of PUUV-Pa, overlaid with agarose medium, incubated for 8 days, fixed, and stained with polyclonal convalescent-phase serum (which detects all substrains of PUUV) or MAb 1C12 (which does not detect PUUV-Sm). The number of focuses detected using the different detection antibodies was then compared. Approximately 9% of infectious viruses in PUUV-Pa were not detected by MAb 1C12. As other substrains also might not be recognized by MAb 1C12, this suggests that maximally 9% of the viruses in PUUV-Pa are represented by PUUV-Sm.

PUUV-La replicates to higher titers than PUUV-Sm in Vero E6 cells. As PUUV-La caused larger focuses than PUUV-Sm on Vero E6 cells, we compared the growth kinetics of the two substrains and the original PUUV-Pa in Vero E6 cells. Cells were infected with 100, 1,000, or 10,000 FFU/well of PUUV-La, PUUV-Sm, or PUUV-Pa. Supernatants were collected at day 2, 4, and 7 postinfection (p.i.), and virus titers were subsequently determined. Generally, PUUV-La produced higher progeny virus titers than PUUV-Sm and PUUV-Pa (Fig. 4A to C). At day 7 p.i., titers in supernatants from PUUV-La-in-

TABLE 3. Hantavirus RdRp sequences from amino acids 691 to 710[a]

Virus	RdRp sequence (aa 691 to 710)[b]
PUUV-Pa	DQSTIGASGVYPSLMSRVVY
PUUV-La	DQSTIGASGVYS**S**LMSRVVY
PUUV-Sm	DQSTIGASGVYPSLMSRVVY
PUUV Sotkamo	DQSTIGASGVYPSLMSRVVY
PUUV Umeå	DQSTIGASGVYPSLMSRVIY
ANDV	DHSTVGASGVYPSLMSRVVY
SNV	DHSTVGASGVYPSLMSRVVY
HTNV	DQSTVGASGVYPSFMSRIVY
SEOV	DQSTVGASGIYPSFMSRVVY

[a] Sequences were obtained from GenBank (accession numbers shown in parentheses) as follows: PUUV-Pa (PUUV strain Kazan; accession no. ABN51178), PUUV strain Sotkamo (NP_942587), PUUV strain Umeå (AAS19472), ANDV (NP_604473), SNV (AAC42204), HTNV (NP_941982), and SEOV (NP_942558).

[b] The mutation observed in PUUV-La RdRp is shown in boldface type.

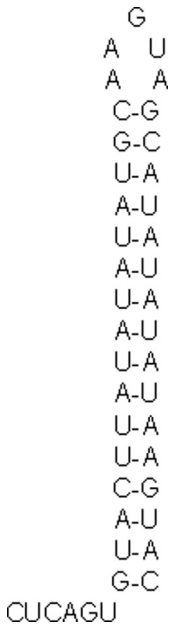

FIG. 2. The PUUV S-segment 5′ NCR contains a predicted hairpin loop. The 43-nucleotide deletion observed in PUUV-La S-segment 5′ NCR forms a hairpin loop that is conserved among Arvicolinae-borne hantaviruses.

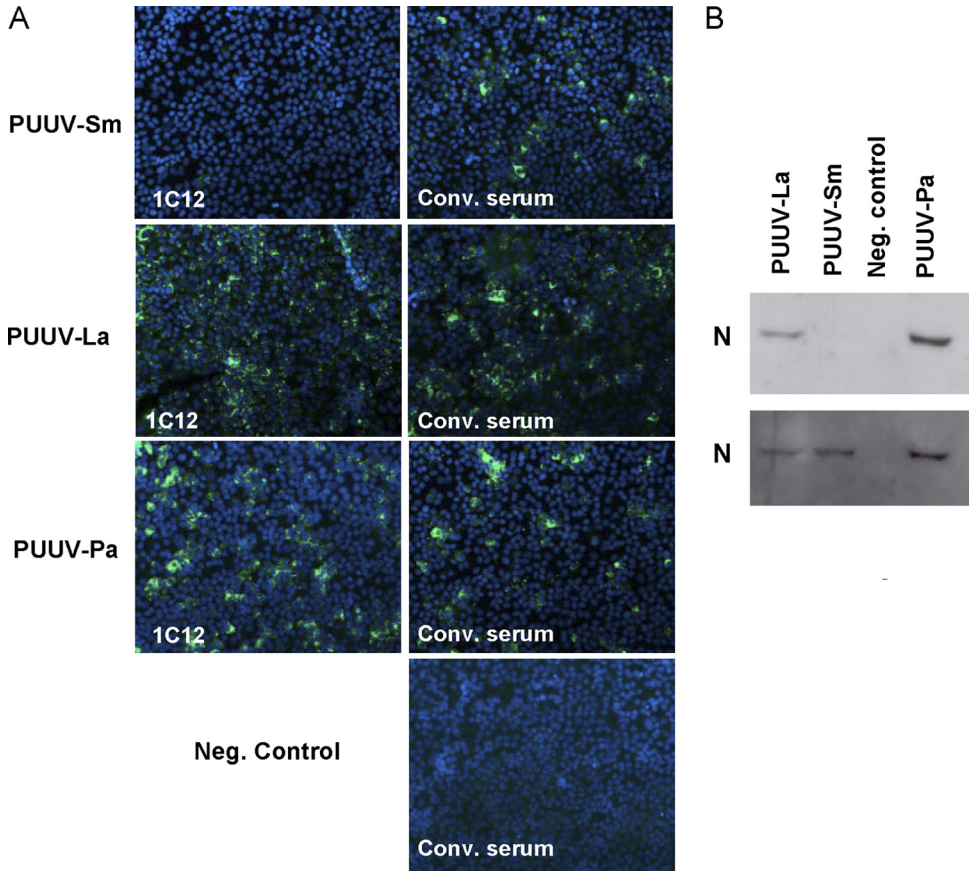

FIG. 3. The D35 amino acid in PUUV N protein is important for recognition by MAb 1C12. (A) MAb 1C12 fails to detect PUUV-Sm-infected Vero E6 cells by immunofluorescence microscopy, while a convalescent-phase anti-PUUV human serum (Conv. serum) does. The cells were counterstained with DAPI. Neg. control, negative control. (B) Western blot analysis of N protein. The gel was loaded with 750 FFU of either PUUV-Sm, PUUV-La, or PUUV-Pa and first stained with MAb 1C12, followed by stripping of the gel and subsequent staining with polyclonal convalescent-phase serum. The N protein of PUUV-La and PUUV-Pa, but not of PUUV-Sm, is detected by the N-protein-specific MAb 1C12 in the Western blot (top gel), while PUUV-Sm N protein, like PUUV-La and PUUV-Pa N protein, is detected by polyclonal convalescent-phase serum (bottom gel).

fected cells were above 2,000,000 FFU/ml regardless of the amount of virus used to initially infect the cells (Fig. 4A to C), while the highest titer observed at day 7 p.i. from PUUV-Sm-infected cells was 544,000 FFU (Fig. 4A to C). This shows that even in cells infected with 100 FFU of PUUV-La, more virus is produced than in cells initially infected with 10,000 FFU of PUUV-Sm. Furthermore, the results show that PUUV-La replicates to higher titers and PUUV-Sm replicates to lower titers than PUUV-Pa in Vero E6 cells.

PUUV-La has a lower ratio of viral RNA to infectious particles than PUUV-Sm and PUUV-Pa. One possible explanation for the observed higher progeny virus production after PUUV-La infection might be that replication of this substrain is more efficient than replication of PUUV-Sm and PUUV-Pa. This possibility was analyzed by comparing the ratios between noninfectious particles (that contain viral RNA but cannot infect cells) and infectious particles in the viral stocks. The ratio between total PUUV S genomic RNA and infectious virus was 2.3-fold higher for PUUV-Sm and 1.9-fold higher for PUUV-Pa than for PUUV-La, suggesting that PUUV-La indeed produces more infectious replication-competent particles than PUUV-Sm and PUUV-Pa per total amount of particles produced.

PUUV-Sm and PUUV-La replicate more efficiently than PUUV-Pa on MRC-5 cells. Possible mutations that would lead to activation of innate immune responses and/or to decreased potential to inhibit activated IFN responses in infected cells will not be strongly selected against in Vero E6 cells, as this cell line lacks the capacity to produce IFN-α and IFN-β (7). In order to analyze whether there were any differences in replication on IFN-α/β-competent cells between the substrains, we infected human embryonic fibroblast MRC-5 cells and analyzed progeny virus production and levels of S-segment RNA in the infected cells over time. Cells were infected with 80,000 FFU of PUUV-La, PUUV-Sm, or PUUV-Pa, and samples were taken at 2, 4, and 7 days p.i.

Surprisingly, we observed that from 4 days p.i. cells infected with PUUV-Pa produced less progeny virus than PUUV-La- and PUUV-Sm-infected cells ($P < 0.001$, factorial ANOVA) (Fig. 5). Furthermore, in contrast to what was observed for Vero E6 cells, we observed similar levels of progeny virus production by PUUV-La- and PUUV-Sm-infected MRC-5

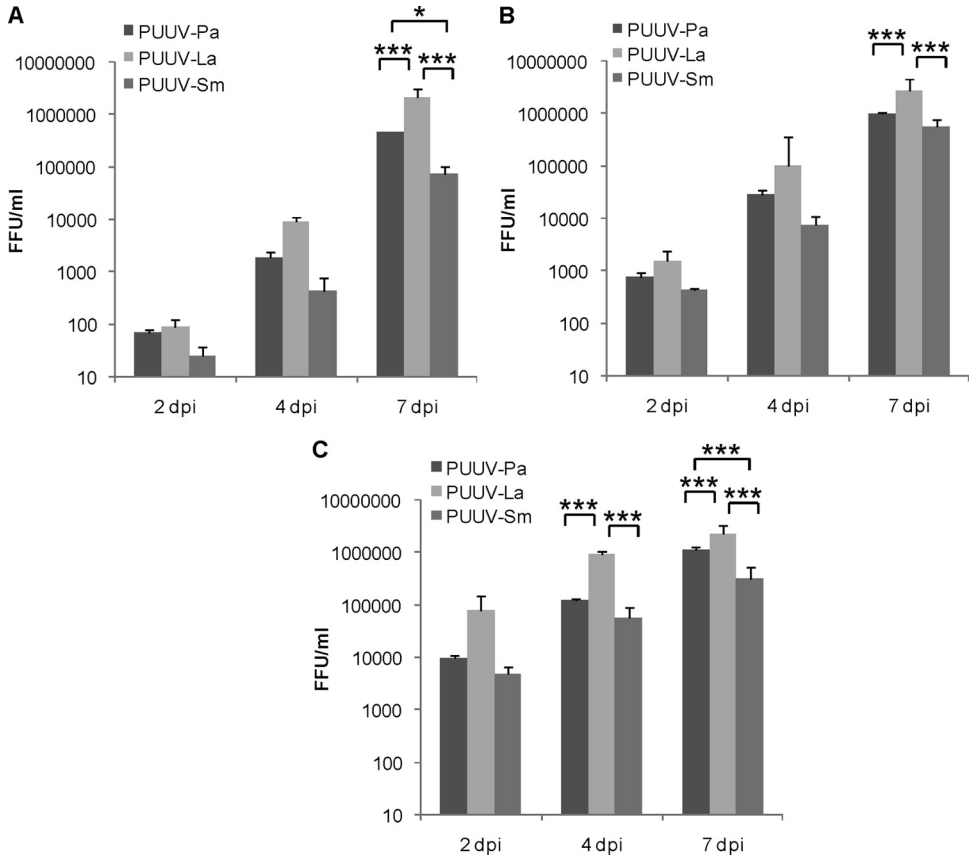

FIG. 4. PUUV-La replicates to higher levels than PUUV-Sm and PUUV-Pa in Vero E6 cells. Vero E6 cells in 24-well plates were infected with 100 focus-forming units (FFU) (A), 1,000 FFU (B), or 10,000 FFU (C) of PUUV-Pa, PUUV-La, or PUUV-Sm. The levels or titers of progeny (in focus-forming units per ml [FFU/ml]) were determined in supernatants taken from infected cells at the indicated time points (days postinfection [dpi]). The values are means plus standard deviations (SDs) (error bars) from three independent experiments. Values that are significantly different as determined by factorial ANOVA are indicated by asterisks and brackets as follows: *, $P < 0.05$; ***, $P < 0.001$.

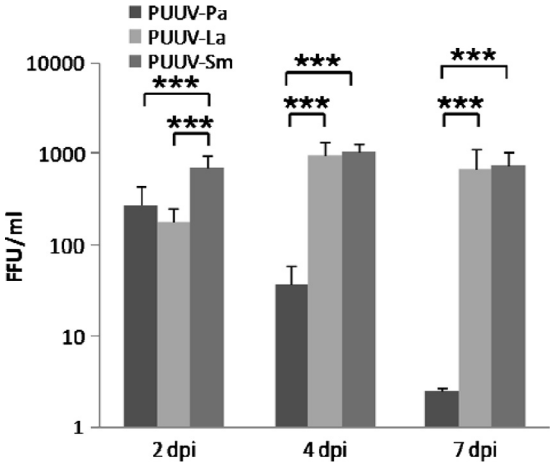

FIG. 5. PUUV-Pa replication is inhibited in MRC-5 cells. MRC-5 cells were infected with 80,000 FFU of PUUV-Pa, PUUV-La, or PUUV-Sm. At the indicated time points (days postinfection [dpi]), supernatants were taken, and the levels of infectious virus particles (in focus-forming units per ml [FFU/ml]) were determined. The values are means plus standard deviations (SDs) (error bars) from two independent experiments. Values that are significantly different ($P < 0.001$) as determined by factorial ANOVA are indicated by brackets and three asterisks.

cells over time (Fig. 5). Production of PUUV-Pa progeny virus clearly decreased over time, and almost no PUUV-Pa progeny virus was detected at 7 days p.i. (Fig. 5). Compared to the titers in supernatants from PUUV-Pa-infected cells, we observed 1.5-fold-lower (PUUV-La) and 2.6-fold-higher (PUUV-Sm) titers at day 2 p.i., 26-fold-higher (PUUV-La) and 28-fold-higher (PUUV-Sm) titers at day 4 p.i., and 270-fold-higher (PUUV-La) and 300-fold-higher (PUUV-Sm) titers at day 7 p.i.

The levels of viral RNA in the infected cells did not differ much for the isolates. Except for PUUV-La-infected cells at day 7 p.i. (2.15-fold-higher level of viral RNA compared to PUUV-Pa-infected cells), we did not observe 2-fold or higher differences in the levels of viral RNA for the three different PUUV isolates at any time point (data not shown).

PUUV-Pa induces stronger innate immune responses than PUUV-La and PUUV-Sm. The results on MRC-5 cells showed that both PUUV-Sm and PUUV-La produce higher levels of progeny virus than PUUV-Pa in IFN-competent MRC-5 cells, despite rather small differences in intracellular viral RNA levels. Furthermore, the decreased progeny virus production over time observed in PUUV-Pa-infected MRC-5 cells (Fig. 5) suggested that PUUV-Pa replication was inhibited by cellular factors.

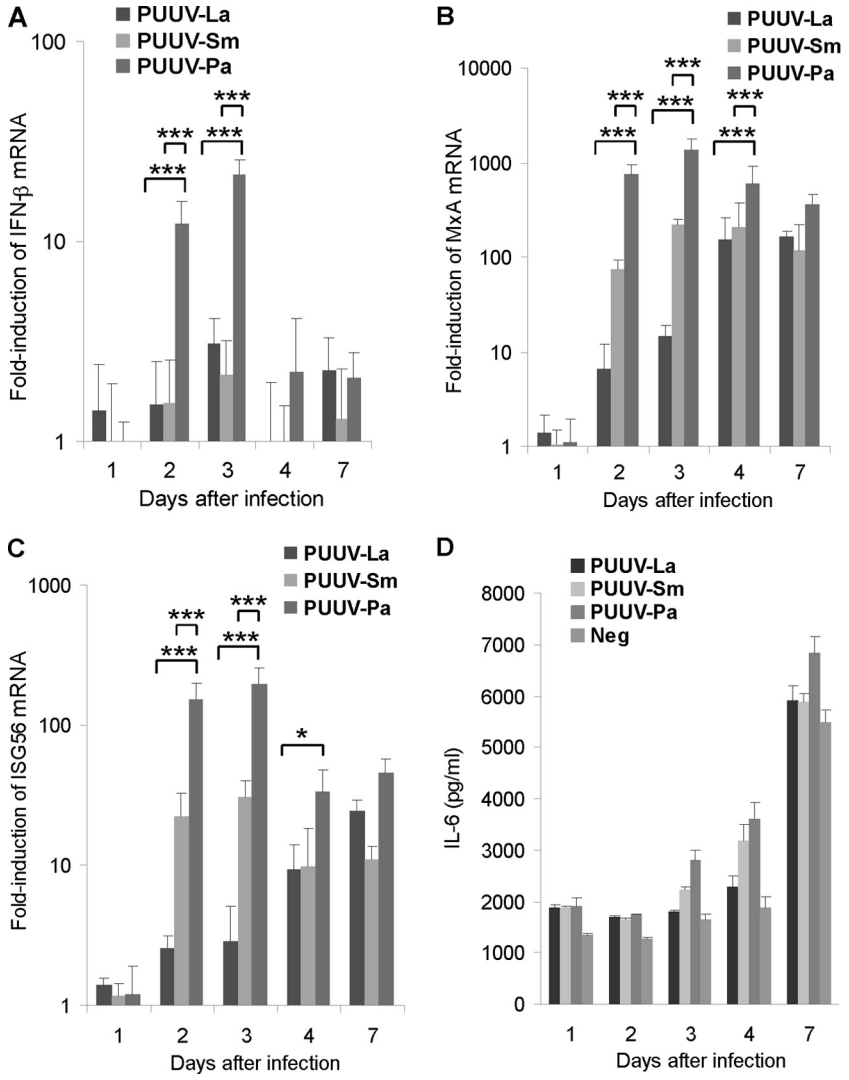

FIG. 6. PUUV-Pa induces stronger innate immune responses in MRC-5 cells than PUUV-La and PUUV-Sm. MRC-5 cells were infected with 80,000 FFU (corresponding to a multiplicity of infection [MOI] of 0.8) of PUUV-Pa, PUUV-La, or PUUV-Sm or left uninfected as a control. The levels of IFN-β (A), MxA (B), and ISG56 (C) mRNA expression in infected cells were determined by Q-PCR at the indicated time points after infection. Data were normalized to β-actin data and presented as relative expression compared to the noninfected control. The values in panels A to C are means plus standard deviations (SDs) (error bars) from two independent experiments. Values that are significantly different as determined by factorial ANOVA are indicated by brackets and asterisks as follows: *, $P < 0.05$; ***, $P < 0.001$. (D) The levels of IL-6 in supernatants at indicated time points after infection were determined in enzyme-linked immunosorbent assays (ELISAs). The values in panel D are means plus standard deviations (SDs) (error bars) from one experiment. Neg, negative control.

Therefore, next we examined the potential of the three isolates to induce innate immune responses in MRC-5 cells. We analyzed the levels of IFN-β, ISG56, and MxA mRNA as markers of induction of innate immune responses. ISG56 can be induced both by virus directly or via IFNs, while MxA is induced only by type I and III IFNs (19). We also analyzed the levels of interleukin 6 (IL-6) in supernatants as a marker of induction of proinflammatory responses.

Generally, PUUV-Pa induced higher levels of IFN-β, ISG56, and MxA transcription in infected cells than PUUV-La and PUUV-Sm (Fig. 6A to C). Induction of IFN-β, MxA, or ISG56 was not observed in infected cells at 1 day p.i. (Fig. 6A to C). IFN-β was clearly induced (>2-fold induction) in PUUV-Pa-infected cells (12-fold induction), but not in PUUV-La- or PUUV-Sm-infected cells, at day 2 p.i.. For PUUV-Pa-infected cells, IFN-β mRNA levels peaked at 3 days p.i. (21-fold induction) and then remained slightly elevated until 7 days p.i. (2.2-fold induction at 4 days p.i. and 2.1-fold induction at 7 days p.i.) (Fig. 6A). PUUV-La and PUUV-Sm showed slightly induced levels of IFN-β at 3 days p.i. (3.1-fold induction for PUUV-La and 2.2-fold induction for PUUV-Sm), and the levels of IFN-β mRNA were also slightly elevated in PUUV-La-infected cells at 7 days p.i. (2.3-fold induction) (Fig. 6A).

MxA was induced from 2 days p.i. in all infected cells (Fig. 6B), and from this time point until 7 days p.i., the level of MxA mRNA was clearly the highest in PUUV-Pa-infected cells, peaking at 3 days p.i. (1,380-fold induction). The level of MxA mRNA peaked at day 7 p.i. in PUUV-La-infected cells (166-

fold induction) and at day 3 p.i. in PUUV-Sm-infected cells (219-fold induction) (Fig. 6B).

ISG56 transcription was clearly induced in PUUV-Pa (152-fold induction) and in PUUV-Sm-infected cells (22.3-fold induction), slightly induced (2.6-fold induction) in PUUV-La-infected cells at day 2 p.i., and then remained elevated until day 7 p.i. (Fig. 6C). The levels of ISG56 mRNA peaked at day 3 p.i. for PUUV-Pa-infected cells (195-fold induction) and PUUV-Sm-infected cells (30.6-fold induction) and at day 7 p.i. for PUUV-La-infected cells (24.6-fold induction) (Fig. 6C).

In general, higher levels of IL-6 were detected in supernatants from PUUV-infected MRC-5 cells than from noninfected cells (Fig. 6D). When comparing the abilities of the different viruses to activate IL-6 production, we observed similar levels of IL-6 in the supernatants from PUUV-La-, PUUV-Sm-, and PUUV-Pa-infected cells the first 2 days after infection (Fig. 6D). At day 3 and 4 p.i., the levels of IL-6 were highest in supernatants from PUUV-Pa-infected cells, second highest in supernatants from PUUV-Sm-infected cells, and lowest in supernatants from PUUV-La-infected cells (Fig. 6D). At day 7 p.i., the levels of IL-6 were similar in supernatants from PUUV-La- and PUUV-Sm-infected cells and clearly higher in supernatants from PUUV-Pa-infected cells (Fig. 6D). These results suggest that PUUV-Pa, at late time points after infection, causes stronger IL-6 responses than PUUV-La and PUUV-Sm.

DISCUSSION

Hantaviruses cause two diseases in humans: HFRS in Europe and Asia and HCPS in the Americas (47, 51). The hantaviruses causing HFRS and HCPS are maintained in the environment by rodents, with humans serving as incidental hosts that are typically infected by inhalation of virus-contaminated rodent excreta. Except for Andes virus (11), no human-to-human transmission seems to occur. At the present time, there is no reverse genetics system available for hantaviruses. Furthermore, *in vitro* studies with hantaviruses are hampered by the fact that hantaviruses are notoriously difficult to isolate, and as only cell line-adapted hantaviruses are used for *in vitro* studies, the number of hantavirus strains in use is very low. Hantaviruses are single-stranded RNA viruses, with an estimated mutation rate similar to other RNA viruses (41). The phenotypic change leading to cell line adaptation of wild-type PUUV is associated with several mutations (37), and an I551T mutation in Gn alters the phenotype of cell line-adapted Hantaan virus (10), clearly showing that spontaneous mutations can have strong effects on the phenotype. The Vero E6 cell line is the most commonly used cell line for adaptation and later growth of hantaviruses. This cell line can produce IFN-λ (39, 49) but is IFN-α/β incompetent (7) and therefore can induce only weak antiviral responses. The interplay between virus and innate immune responses, especially the IFN-α/β-dependent antiviral responses, is normally crucial in determining the outcome of an infection (14). As hantaviruses are passaged on Vero E6 cells, natural mutations, which will give raise to virus variants that in a natural setting (i.e., in the natural host) normally would be selected against, are likely to evolve. In naturally infected hosts, hantaviruses also mutate and quasispecies are frequently detected (12, 44, 45). However, as the natural hosts have intact and functional immune responses, it can be expected that virus variants that are readily detected by the immune system or are directly pathogenic are selected against, and therefore, not all of the observed quasispecies survive over time. As cell line-adapted hantaviruses are used for infectious experiments, it can be speculated that observed results might partly be dependent on the different substrains that constitute the virus stock in use. Here, we have analyzed possible phenotypic differences between two substrains, PUUV-La and PUUV-Sm, isolated from PUUV-Pa and between the two substrains and PUUV-Pa.

We observed one amino acid mutation in the PUUV-La N protein and another one in the PUUV-Sm N protein. Hantavirus N protein contains 429 to 433 amino acids and is involved in several processes (21). It is an RNA chaperone (34) that can form homodimers and homotrimers and bind to viral RNA, forming capsids that are incorporated into virus particles (21). The N protein is also required for viral RNA synthesis (13) and is involved in the cap-snatching process required for successful hantavirus RNA replication (36). The N protein can substitute for the entire cellular eIF4F complex, and preferentially bind mRNA encoded by hantavirus genes to ribosomes, thereby increasing the amount of hantavirus proteins produced in the infected cell (35). The N protein has been suggested to inhibit tumor necrosis factor (TNF)-induced activation of NF-κB via interaction with importin α (50) and by direct binding of NF-κB (38). The N protein also binds to actin (43), Daxx (29), and SUMO-1-related proteins (28) and might be transported on microtubules in a dynein-dependent fashion (40). This shows that the N protein is involved in, and therefore potentially can interfere with, several cellular functions. The secondary structure of the first 70 amino acids in the N protein has been solved (3, 6, 52). From these reports, it has been suggested that PUUV N-protein D27 is located within α-helix 1, while D35 is on the apex formed between α-helix 1 and α-helix 2. For Tula virus, it has been suggested that D35, D38, L44, V51, E55, L58, and R63 in the N protein are important for N-protein interaction and dimerization (3, 4). Our data show that D27 and D35 are not required for PUUV replication.

We also observed one amino acid mutation in the PUUV-La RdRp and another one in the PUUV-Sm RdRp. It remains to be shown whether the mutations observed in N protein and RdRp are connected to each other or not. Hantavirus RdRp is a large protein of approximately 250 kDa (26, 27). Whether hantavirus RdRp has functions other than transcriptase and replicase activity is currently not known. Rift Valley fever virus RdRp forms an oligomer; this formation is dependent on the amino acid residues SDD and is required for polymerase activity (53). The RdRp SDD motif is conserved among all segmented negative-stranded RNA viruses, suggesting that hantavirus RdRp might also form biologically active oligomers. The mutation frequency in the PUUV L segment is higher than in the S and M segments (44). None of the mutations observed in this study are in the proposed functional domains of RdRp (27), and it remains to be shown whether these mutations in any way alter the enzymatic, or any other, function of RdRp.

Deletions in the NCR regions of Seoul virus (SEOV) S, M, and L RNA have been observed to accumulate over time after infection, with up to 39 nucleotide deletions in the NCR of S

(33). However, these deletions were detected in cRNA and not in viral RNA (vRNA) (33). In a report by Kukkonen and coworkers, it was shown that the Tula virus termini of S and L segments are heterogeneous, with 1- to 22-nt deletions or 1 to 3 extra nucleotide insertions (25). These deletions and insertions were also observed more often in viral RNA from infected cells than from pelleted virus, indicating that they might represent nonfunctional viral RNA. Our finding of a 43-nucleotide deletion in the S-segment 5′ NCR in viral RNA isolated from viral particles shows that PUUV can successfully replicate in the complete absence of this genomic part. If the hairpin loop structure has any function, for example as a microRNA (miRNA), remains to be shown.

Interestingly, we observed no differences in the M-segment sequences in the two isolates. This strongly suggests that the differences in the observed phenotypes are not explained by possible differences in the function of the Gn and Gc proteins. Gn and Gc are the envelope proteins in virus particles directing entry into cells, and they might also interfere with the activation and function of the antiviral system in infected cells (1, 2, 15, 16, 48). Finding identical M segments indicates that a reassortment between PUUV-La and PUUV-Sm may have occurred and that one of these substrains has picked up the other's M segment. Reassortments are frequently observed for PUUV in the natural hosts, and it seems that there is a nonrandom distribution of genomic segments, with S and L preferentially originating from the same isolate found in the reassortments (45). Cocultivation of Andes and Sin Nombre hantaviruses also resulted in reassortments with homologous S and L segments (46), as did a reassortment between PUUV and Prospect Hill virus containing a PUUV M segment and Prospect Hill virus S and L segments (18). However, our data do not exclude the possibility that the M segment found in PUUV-La and PUUV-Sm is well conserved within or might even represent the only M-segment variant in the different substrains that constitute the PUUV-Pa strain.

We observed that the PUUV-La stock had the lowest ratio of viral RNA to infectious virus particles, suggesting that PUUV-La replicated more efficiently and that PUUV-Sm and PUUV-Pa contained more defective particles per infectious virus than PUUV-La. This finding might explain the observation from the Western blot (Fig. 3B) of a weaker band for N protein in cells grown in wells loaded with 750 FFU of PUUV-La than for cells grown in wells loaded with 750 FFU of PUUV-Pa, as it indicates that the gel was loaded with less PUUV-La protein than PUUV-Pa protein. However, another possible explanation could be that MAb 1C12 is dependent not only on D35 but also on D27 in the N protein for strong binding. Focus-purified PUUV isolates can differ in the ratio of defective particles to infectious particles (17), indicating that there are differences in the effectiveness of viral replication of different isolates. It has been reported that focus isolation of hantaviruses increases titers in stocks obtained from subsequent infections, indicating that purified hantaviruses replicate with higher efficacy than the mixed parental strains (42). In contrast, PUUV-La and PUUV-Sm showed different capacities to produce progeny virus in Vero E6 cells, showing that focus purification does not always lead to increased viral production.

In order to study activation of innate immune responses, we analyzed induction of ISG56, MxA, and IFN-β and production of IL-6 in MRC-5 cells. PUUV-Pa induced stronger innate immune responses than PUUV-La and PUUV-Sm, and PUUV-Sm induced stronger responses than PUUV-La. We observed similar levels of viral RNA in PUUV-La-, PUUV-Sm-, and PUUV-Pa-infected MRC-5 cells but lower production of progeny virus after PUUV-Pa infection. Therefore, it seems likely that the early induction of IFN-β and the strong induction of MxA and ISG56 observed in PUUV-Pa-infected cells are not explained by increased viral RNA production. When combining the data obtained from Vero E6 and MRC-5 cells, it seems that PUUV-Pa has a disadvantage on IFN-competent cells, but not on Vero E6 cells that cannot produce type I IFNs. A possible explanation could be that PUUV-Pa induces stronger IFN responses than PUUV-La and PUUV-Sm.

Why would PUUV-Pa induce a stronger innate immune response than PUUV-La and PUUV-Sm? PUUV-Pa consists of a mixture of isolates. We do not know the exact composition of the different substrains in PUUV-Pa or how many substrains are represented in PUUV-Pa. In theory, even if only a minority of the viruses constituting PUUV-Pa induce strong innate immune responses, the minority might cause the IFN responses observed in MRC-5 cells. If so, while a majority of the substrains within PUUV-Pa probably induce weak IFN responses, like PUUV-La and PUUV-Sm, a small proportion of the viruses might induce strong innate immune responses, and therefore be responsible for the overall antiviral effect observed in MRC-5 cells. This activation would also have a negative impact on substrains that do not induce strong IFN responses, and consequently, progeny virus production would be inhibited.

In conclusion, we report that the phenotypes of two substrains of hantavirus generated from the same parental strain can show substantial differences from each other and from the original strain. This shows that natural mutations, accumulating during propagation of hantavirus, can have considerable effects on the overall phenotype. Importantly, this suggests that phenotypic differences *in vitro* reported for hantaviruses might depend more on chance due to mutations during passage than due to true inherited differences between different hantaviruses.

ACKNOWLEDGMENTS

This work was supported by Åke Wibergs Stiftelse, Magn. Bergvalls Stiftelse, Jeanssons Stiftelse, Stiftelsen Clas Groschinskys Minnesfond, the Swedish Society of Medicine, the Royal Swedish Academy of Sciences, and the Swedish Medical Research Council.

REFERENCES

1. **Alff, P. J., et al.** 2006. The pathogenic NY-1 hantavirus G1 cytoplasmic tail inhibits RIG-I- and TBK-1-directed interferon responses. J. Virol. **80:**9676–9686.
2. **Alff, P. J., N. Sen, E. Gorbunova, I. N. Gavrilovskaya, and E. R. Mackow.** 2008. The NY-1 hantavirus Gn cytoplasmic tail coprecipitates TRAF3 and inhibits cellular interferon responses by disrupting TBK1-TRAF3 complex formation. J. Virol. **82:**9115–9122.
3. **Alminaite, A., V. Backström, A. Vaheri, and A. Plyusnin.** 2008. Oligomerization of hantaviral N protein: charged residues in the N-terminal coiled-coil domain contribute to intermolecular interactions. J. Gen. Virol. **89:**2167–2174.
4. **Alminaite, A., et al.** 2006. Oligomerization of hantavirus N protein: analysis of the N-terminal coiled-coil domain. J. Virol. **80:**9073–9081.
5. **Arai, S., et al.** 2008. Molecular phylogeny of a newfound hantavirus in the

Japanese shrew mole (Urotrichus talpoides). Proc. Natl. Acad. Sci. U. S. A. **105:**16296–16301.
6. **Boudko, S. P., R. J. Kuhn, and M. G. Rossmann.** 2007. The coiled-coil domain structure of the Sin Nombre virus N protein. J. Mol. Biol. **366:**1538–1544.
7. **Diaz, M. O., et al.** 1988. Homozygous deletion of the α- and β1-interferon genes in human leukemia and derived cell lines. Proc. Natl. Acad. Sci. U. S. A. **85:**5259–5263.
8. **Do, C. B., D. A. Woods, and S. Batzoglou.** 2006. CONTRAfold: RNA secondary structure prediction without physics-based models. Bioinformatics **22:**e90–98.
9. **Easterbrook, J. D., and S. L. Klein.** 2008. Immunological mechanisms mediating hantavirus persistence in rodent reservoirs. PLoS Pathog. **4:**e1000172.
10. **Ebihara, H., et al.** 2000. Pathogenicity of Hantaan virus in newborn mice: genetic reassortant study demonstrating that a single amino acid change in glycoprotein G1 is related to virulence. J. Virol. **74:**9245–9255.
11. **Ferres, M., et al.** 2007. Prospective evaluation of household contacts of persons with hantavirus cardiopulmonary syndrome in Chile. J. Infect. Dis. **195:**1563–1571.
12. **Feuer, R., J. D. Boone, D. Netski, S. P. Morzunov, and S. C. St. Jeor.** 1999. Temporal and spatial analysis of Sin Nombre virus quasispecies in naturally infected rodents. J. Virol. **73:**9544–9554.
13. **Flick, K., et al.** 2003. Rescue of Hantaan virus minigenomes. Virology **306:**219–224.
14. **García-Sastre, A., and C. A. Biron.** 2006. Type 1 interferons and the virus-host relationship: a lesson in détente. Science **312:**879–882.
15. **Geimonen, E., et al.** 2003. Hantavirus pulmonary syndrome-associated hantaviruses contain conserved and functional ITAM signaling elements. J. Virol. **77:**1638–1643.
16. **Geimonen, E., et al.** 2002. Pathogenic and nonpathogenic hantaviruses differentially regulate endothelial cell responses. Proc. Natl. Acad. Sci. U. S. A. **99:**13837–13842.
17. **Handke, W., D. H. Krüger, and A. Rang.** 2009. Defective particles can lead to underestimated antibody titers in virus neutralization tests. Intervirology **52:**335–339.
18. **Handke, W., et al.** 2010. Generation and characterization of genetic reassortants between Puumala and Prospect Hill hantavirus in vitro. J. Gen. Virol. **91:**2351–2359.
19. **Holzinger, D., et al.** 2007. Induction of MxA gene expression by influenza A virus requires type I or type III interferon signaling. J. Virol. **81:**7776–7785.
20. **Jääskeläinen, K. M., et al.** 2007. Tula and Puumala hantavirus NSs ORFs are functional and the products inhibit activation of the interferon-beta promoter. J. Med. Virol. **79:**1527–1536.
21. **Kaukinen, P., A. Vaheri, and A. Plyusnin.** 2005. Hantavirus N protein: a multifunctional molecule with both housekeeping and ambassadorial duties. Arch. Virol. **150:**1693–1713.
22. **Khaiboullina, S. F., A. A. Rizvanov, V. M. Deyde, and S. C. St. Jeor.** 2005. Andes virus stimulates interferon-inducible MxA protein expression in endothelial cells. J. Med. Virol. **75:**267–275.
23. **Klingström, J., M. Stoltz, J. Hardestam, C. Ahlm, and Å. Lundkvist.** 2008. Passive immunization protects cynomolgus macaques against Puumala hantavirus challenge. Antivir. Ther. **13:**125–133.
24. **Klingström, J., et al.** 2006. Nitric oxide and peroxynitrite have different antiviral effects against hantavirus replication and free mature virions. Eur. J. Immunol. **36:**2649–2657.
25. **Kukkonen, S. K., A. Vaheri, and A. Plyusnin.** 1998. Completion of the Tula hantavirus genome sequence: properties of the L segment and heterogeneity found in the 3′ termini of S and L genome RNAs. J. Gen. Virol. **79:**2615–2622.
26. **Kukkonen, S. K., A. Vaheri, and A. Plyusnin.** 2004. Tula hantavirus L protein is a 250 kDa perinuclear membrane-associated protein. J. Gen. Virol. **85:**1181–1189.
27. **Kukkonen, S. K., A. Vaheri, and A. Plyusnin.** 2005. L protein, the RNA-dependent RNA polymerase of hantaviruses. Arch. Virol. **150:**533–556.
28. **Lee, B. H., et al.** 2003. Association of the N protein of the Seoul and Hantaan hantaviruses with small ubiquitin-like modifier-1-related molecules. Virus Res. **98:**83–91.
29. **Li, X. D., et al.** 2002. Hantavirus nucleocapsid protein interacts with the Fas-mediated apoptosis enhancer Daxx. J. Gen. Virol. **83:**759–766.
30. **Lundkvist, Å., A. Fatouros, and B. Niklasson.** 1991. Antigenic variation of European haemorrhagic fever with renal syndrome virus strains characterized using bank vole monoclonal antibodies. J. Gen. Virol. **72:**2097–2103.
31. **Lundkvist, Å., et al.** 1997. Cell culture adaptation of Puumala hantavirus changes the infectivity for its natural reservoir, *Clethrionomys glareolus*, and leads to accumulation of mutants with altered genomic RNA S segment. J. Virol. **71:**9515–9523.
32. **Mackow, E. R., and I. N. Gavrilovskaya.** 2009. Hantavirus regulation of endothelial cell functions. Thromb. Haemost. **102:**1030–1041.
33. **Meyer, B. J., and C. Schmaljohn.** 2000. Accumulation of terminally deleted RNAs may play a role in Seoul virus persistence. J. Virol. **74:**1321–1331.
34. **Mir, M. A., and A. T. Panganiban.** 2006. The bunyavirus N protein is an RNA chaperone: possible roles in viral RNA panhandle formation and genome replication. RNA **12:**272–282.
35. **Mir, M. A., and A. T. Panganiban.** 2008. A protein that replaces the entire cellular eIF4F complex. EMBO J. **27:**3129–3139.
36. **Mir, M. A., W. A. Duran, B. Hjelle, C. Ye, and A. T. Panganiban.** 2008. Storage of cellular 5′ mRNA caps in P bodies for viral cap-snatching. Proc. Natl. Acad. Sci. U. S. A. **105:**19294–19299.
37. **Nemirov, K., Å. Lundkvist, A. Vaheri, and A. Plyusnin.** 2003. Adaptation of Puumala hantavirus to cell culture is associated with point mutations in the coding region of the L segment and in the noncoding regions of the S segment. J. Virol. **77:**8793–8800.
38. **Ontiveros, S. J., Q. Li, and C. B. Jonsson.** 2010. Modulation of apoptosis and immune signaling pathways by the Hantaan virus N protein. Virology **401:**165–178.
39. **Prescott, J., et al.** 2010. New world hantavirus activate IFNl production in type I IFN-deficient Vero E6 cells. PLoS One **5:**e11159.
40. **Ramanathan, H. N., et al.** 2007. Dynein-dependent transport of the hantaan virus N protein to the endoplasmic reticulum-Golgi intermediate compartment. J. Virol. **81:**8634–8647.
41. **Ramsden, C., F. L. Melo, L. M. Figueiredo, E. C. Holmes, and P. M. Zanotto.** 2008. High rates of molecular evolution in hantaviruses. Mol. Biol. Evol. **25:**1488–1492.
42. **Rang, A., H. Heider, R. Ulrich, and D. H. Krüger.** 2006. A novel method for cloning of non-cytolytic viruses. J. Virol. Methods **135:**26–31.
43. **Ravkov, E. V., S. T. Nichol, C. J. Peters, and R. W. Compans.** 1998. Role of actin microfilaments in Black Creek Canal virus morphogenesis. J. Virol. **72:**2865–2870.
44. **Razzauti, M., A. Plyusnina, H. Henttonen, and A. Plyusnin.** 2008. Accumulation of point mutations and reassortment of genomic RNA segments are involved in the microevolution of Puumala hantavirus in a bank vole (Myodes glareolus) population. J. Gen. Virol. **89:**1649–1660.
45. **Razzauti, M., A. Plyusnina, T. Sironen, H. Henttonen, and A. Plyusnin.** 2009. Analysis of Puumala hantavirus in a bank vole population in northern Finland: evidence for co-circulation of two genetic lineages and frequent reassortment between strains. J. Gen. Virol. **90:**1923–1931.
46. **Rizvanov, A. A., S. F. Khaiboullina, and S. St. Jeor.** 2004. Development of reassortant viruses between pathogenic hantavirus strains. Virology **327:**225–232.
47. **Schönrich, G., et al.** 2008. Hantavirus-induced immunity in rodent reservoirs and humans. Immunol. Rev. **225:**163–189.
48. **Spiropoulou, C. F., C. G. Albariño, T. G. Ksiazek, and P. E. Rollin.** 2007. Andes and Prospect Hill hantaviruses differ in early induction of interferon although both can downregulate interferon signaling. J. Virol. **81:**2769–2776.
49. **Stoltz, M., and J. Klingström.** 2010. Alpha/beta interferon (IFN-alpha/beta)-independent induction of IFN-lambda1 (interleukin-29) in response to Hantaan virus infection. J. Virol. **84:**9140–9148.
50. **Taylor, S. L., N. Frias-Staheli, A. García-Sastre, and C. S. Schmaljohn.** 2009. Hantaan virus N protein binds to importin alpha proteins and inhibits tumor necrosis factor alpha-induced activation of nuclear factor kappa B. J. Virol. **83:**1271–1279.
51. **Vapalahti, O., et al.** 2003. Hantavirus infections in Europe. Lancet Infect. Dis. **3:**653–661.
52. **Wang, Y., et al.** 2008. NMR structure of the N-terminal coiled coil domain of the Andes hantavirus N protein. J. Biol. Chem. **283:**28297–28304.
53. **Zamoto-Niikura, A., K. Terasaki, T. Ikegami, C. J. Peters, and S. Makino.** 2009. Rift valley fever virus L protein forms a biologically active oligomer. J. Virol. **83:**12779–12789.